JOURNAL OF SOLID STATE CHEMISTRY 114, 73–78 (1995)

Synthesis and Structure of Bi_3NF_6: A Member with $n = 3$ of the Vernier Phases M_nX_{2n+1}

M. Hofmann, E. Schweda, and J. Strähle[1]

Institut für Anorganische Chemie der Universität Tübingen, Auf der Morgenstelle 18, D-72076 Tübingen, Germany

J. P. Laval and B. Frit

Laboratoire de Matériaux Céramiques et de Traitements de Surface, URA CNRS no. 320, Université de Limoges, 123 av. A. Thomas, F-87060 Limoges cedex, France

and

M. A. Estermann[2]

ISIS Science Division, Rutherford Appleton Laboratory, Oxfordshire, OXON OX11 0QX, United Kingdom

Received January 20, 1994; in revised form March 23, 1994; accepted March 30, 1994

Heating of NH_4BiF_4 at 285°C under dry ammonia yields Bi_3NF_6 via the intermediate products $NH_4Bi_3F_{10}$ and BiF_3. Bi_3NF_6 is an air-sensitive grey powder decomposing under dry NH_3 at 350°C to form Bi metal. It crystallizes in the orthorhombic space group *Pbcm*, with $a = 581.74(2)$, $b = 570.18(2)$, $c = 1851.13(5)$ pm, $Z = 4$. The structure was determined by X-ray and neutron powder diffraction data. Bi_3NF_6 belongs to the family of vernier phases M_nX_{2n+1}, and represents the first member of the series with $n = 3$. The two-symmetry independent Bi atoms exhibit coordination numbers of eight. © 1995 Academic Press, Inc.

INTRODUCTION

Ammonolysis reactions of ammonium fluorometallates have been shown to yield metal nitride fluorides like TiNF (1), ZrNF (2), $TaNF_2$ (3), and Ln_3NF_6 (4, 5). In dependence of the reaction conditions some oxygen might be introduced into the nitride fluorides, either forming solid solutions as in the case of TiNF and $TaNF_2$ or forming stoichiometric compounds as $Zr_4ON_3F_5$ (2) or $Hf_5ON_4F_6$ (6). We have now also studied the ammonolysis reaction of NH_4BiF_4 which yields Bi_3NF_6 with $NH_4Bi_3F_{10}$ and BiF_3 as intermediate compounds. The ammonolysis of BiF_3 already was investigated (7), resulting in an impure compound with an approximate composition $BiN_{0.34}F_{1.72}O_{0.13}$. Its powder pattern corresponds to the diagram of Bi_3NF_6 with additional reflections of rhombohedral BiO_xF_{3-2x}.

EXPERIMENTAL

Synthesis of Bi_3NF_6

NH_4BiF_4 is heated in a monel tube under an atmosphere of dry and oxygen free NH_3 for 3 hr at 250°C yielding $NH_4Bi_3F_{10}$. Further heating for 30 hours at 285°C under NH_3 affords Bi_3NF_6 which is formed via intermediate BiF_3. Prior to use, NH_3 was condensed over Na, and then slowly evaporated into the reaction tube.

Analysis for Bi_3NF_6: N (found), 1.83%; (calc.), 1.85%; F (found), 14.5%; (calc.): 15.1%; Bi (found), 83.0%; (calc.): 83.05%.

Structure Determination

Comparing the scattering powers of the involved elements for X rays and neutrons clearly indicates that X-ray diffraction data are most suitable to locate the strongly scattering Bi atoms, whereas neutron diffraction data will allow to distinguish unambiguously between F (scattering length: $b = 5.7$ fm) and N atoms ($b = 9.3$ fm).

To find the Bi positions first, integrated intensities for reflections between 8° and 90° in 2Θ (min. d-spacing 110 pm) were extracted from the X-ray powder diffraction pattern with the program FullProf (8). Of the 260 reflections extracted, 117 were within 15% of the full width at half maximum of another reflection, and thus, were considered to be severely overlapping. Equipartitioning of the total intensity of a peak over the contributing, se-

[1] To whom correspondence should be addressed.

[2] Present address: Professur für Kristallographie, ETH Zentrum, CH-8092 Zürich, Switzerland.

0022-4596/95 $6.00

verely overlapping reflections was used to obtain a single-crystal-like data set (9). After the normalization of the intensities with a Wilson plot, a sharpened Patterson function with $|E * F|$ as coefficient was calculated.

Normally, one searches in the Patterson function for the strongest inter atomic vectors, e.g., those vectors between the heavy atoms. The vectors between symmetrically equivalent atomic positions are called Harker vectors $H_{s,t}(\mathbf{r})$ (10):

$$H_{s,t}(\mathbf{r}) = C_s\mathbf{r} - C_t\mathbf{r} = (C_s - C_t)\mathbf{r},$$

C_s = *sth* symmetry operator ($s = 1, \ldots, n$).

Once these Harker vectors are identified in the Patterson function, they can be directly used to infer the original heavy atom position $\mathbf{r}$. In practice, the identification of the Harker vectors depends largely upon the quality of the used Patterson function and the complexity of the structure involved. In the case of powder data, equipartitioning the intensity of overlapping reflections results in a generally "flat" Patterson function with broader peaks and fewer features (9). Consequently, the peak positions are less reliable or may be lost altogether.

In an attempt to overcome these difficulties we employed the symmetry minimum function (SMF)

$$SMF(\mathbf{r}) = \min_{s=1}^{n} \frac{1}{m_s} P(\mathbf{r} - C_s\mathbf{r}),$$

which uses the entire Patterson function and the space-group symmetry rather than just the strongest vectors (11). The SMF searches the Patterson function systematically for large Harker vectors; the quantity m_s takes the multiplicity of the Harker vectors $\mathbf{r} - C_s\mathbf{r}$ into account.

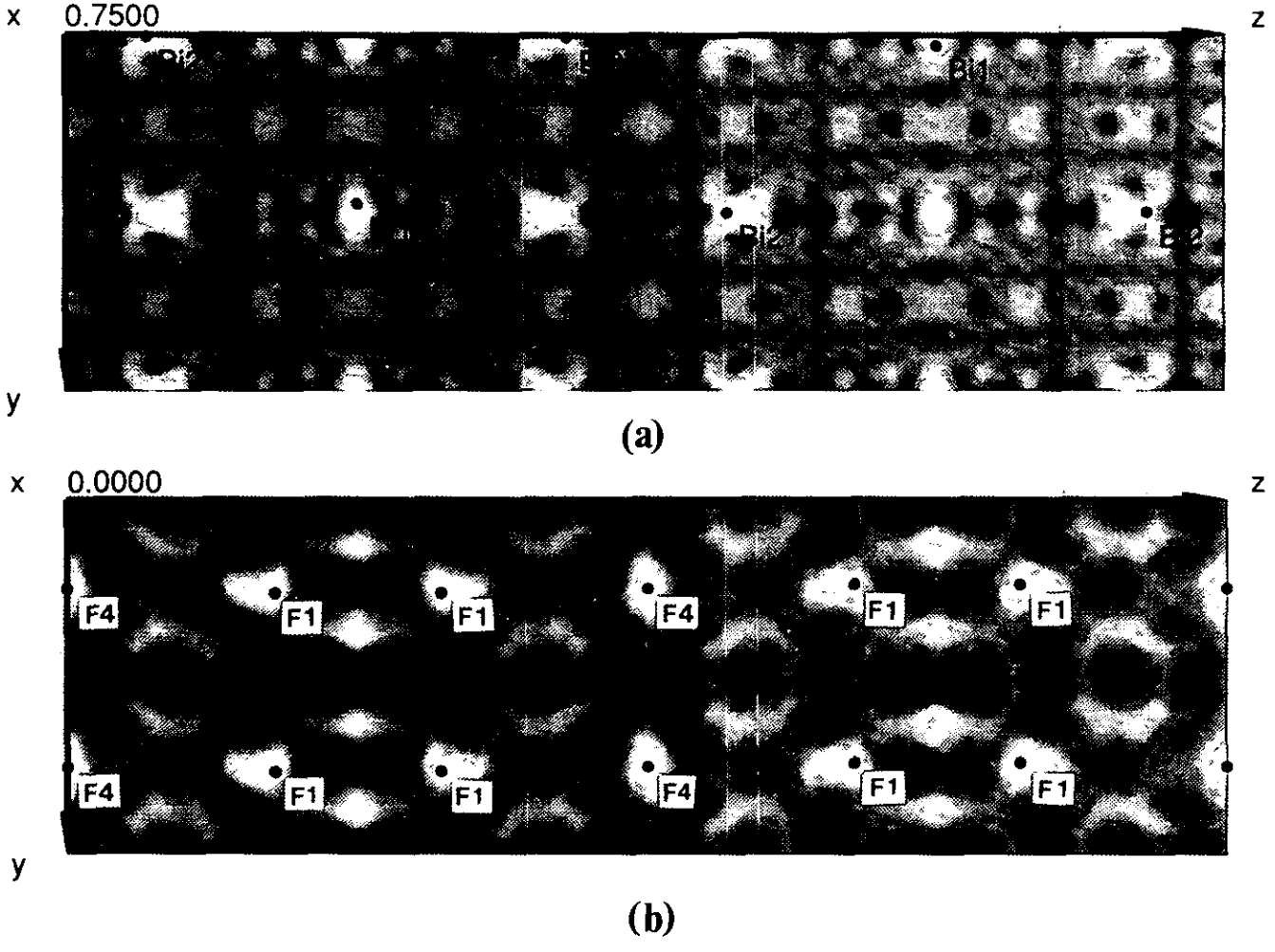

FIG. 1. (a) Section at $x = 0.75$ of the symmetry minimum function (SMF) for Bi_3NF_6. The refined positions of Bi(1) and Bi(2) are indicated in the map. Additional maxima occur by shifting the positions of Bi(1) and Bi(2) by 0, 1/2, 0 and 0, 0, 1/2 (permissible origin shifts). (b) Section at $x = 0.0$ of the image seeking minimum function (IMF) for Bi_3NF_6. The refined positions of the atoms F(1) and F(4) are indicated in the map.

The maxima in the SMF are the possible positions for heavy atoms, including the ones related by a permissible origin shift (Fig. 1a). The position of the strongest peak in the SMF was assigned to the first Bi atom which in turn was input for the image seeking minimum function IMF (11). It systematically searches the Patterson function for large cross-vectors between the first Bi atom at position $\mathbf{r}^*$ and other positions at $\mathbf{r}$,

$$IMF(\mathbf{r}) = \min_{s=1}^{n} P(\mathbf{r} - C_s\mathbf{r}^*).$$

The maxima in the IMF can now directly be related to atomic positions because the origin is fixed with Bi(1). In fact, the second Bi atom and the F and N atoms appeared in the IMF (Fig. 1b).

The atomic positions have then been refined on the basis of the X-ray data with the program FullProf (8). Then, to distinguish between the N and F positions, neutron diffraction powder data have been collected (12) and used for a Rietveld refinement (13) (Fig. 2, Tables 1 and 2).

A bond valence calculation (14) clearly indicated that the anion in position 0.498, 0.25, 0.0 should be nitrogen as a valence sum of 3.06 was obtained while values of 0.78–0.90 resulted for the other four anions which consequently have been assigned to fluorine atoms. This result was confirmed by the Rietveld refinement (13) of the neutron diffraction data which gave R_{wp} values of about 15.0 and unreasonable occupation factors for N in the positions of F(1) to F(4). (Table 2). Refinement with the anions in the positions given in Table 2 converged, how-

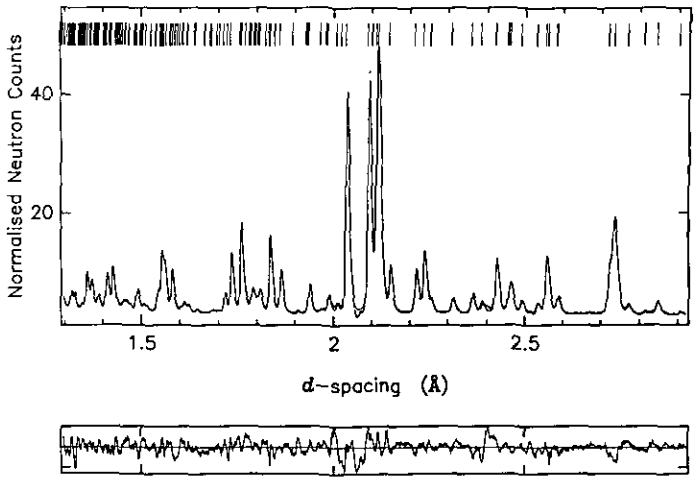

FIG. 2. Observed (dotted line) and calculated (full line) neutron powder diffraction pattern of Bi_3NF_6. The bottom line is the difference pattern.

TABLE 1
Crystal Data and Parameters of the Structure Determination and Refinement

Formula	Bi_3NF_6		
Molar mass	755.25 g/mol		
Space group	*Pbcm*		
Crystal system	orthorhombic		
Cell dimensions	a = 581.74(2) pm		
	b = 570.18(2) pm		
	c = 1851.13(5) = 3 · 617.04 pm		
Volume	$V = 614.01 \cdot 10^6$ pm^3		
Formula units	$Z = 4$		
Density	$\rho_{calc} = 8.165$ g · cm^{-3}		
	X-ray diffraction data	Neutron diffraction data	
		Back scattering	90° detector
Parameters refined	40	38	38
No. of profile points measured	4101	1700	1950
Profile function	Pseudo-Voigt	Voigt	Voigt
Zero point	0.0249(4)		
Scan range		8000–18000 μsec	7500–19000 μsec
Profile parameters (22,23)	U = 0.125(4)	$\sigma(2)$ = 32.276(5)	122.04(2)
	V = −0.050(1)	$\gamma(2)$ = 2.843(1)	1.139(9)
	W = 0.013(7)		
Agreement factors	R_p = 13.2	5.9	5.0
	R_{wp} = 17.9	5.4	4.2
	χ^2 = 2.19	2.45	2.23
	R_{Bragg} = 4.43	3.01	2.05
Expected R-value	R_{exp} = 12.2	3.45	2.80

TABLE 2
Positional Parameters and their Estimated Standard Deviations

Atom	x	y	z	$B(10^{-4}$ pm$^2)$
Bi(1)	0.2207(5)	−0.0296(7)	0.25	0.31(5)
Bi(2)	0.2923(3)	0.5056(6)	0.0688(1)	0.73(2)
F(1)	−0.0180(8)	0.7377(9)	0.6778(1)	1.45(3)
F(2)	0.3716(6)	0.5395(8)	0.8722(2)	1.45(3)
F(3)	0.6046(9)	0.1257(9)	0.25	1.45(3)
F(4)	−0.0118(11)	0.25	0.0	1.45(3)
N	0.4983(9)	0.25	0.0	1.45(3)

Note. The parameters are based on the refinement of the neutron diffraction data.

ever, with reasonable occupation factors and R_{wp} = 5.4 and 4.2 (Table 1).

RESULTS AND DISCUSSION

Synthesis and Properties of Bi_3NF_6

Heating of NH_4BiF_4 under dry NH_3 at 250°C and 285°C leads in first steps to a decomposition to $NH_4Bi_3F_{10}$ and BiF_3 (Eq. [1]) before the ammonolysis proceeds to Bi_3NF_6 (Eq. [2]). $NH_4Bi_3F_{10}$ crystallizes isotypically to cubic KY_3F_{10} (15) in the space group $Fm\bar{3}m$ with a = 1197.60(2) pm:

$$3\ NH_4BiF_4 \xrightarrow[-2NH_4F]{250°C} NH_4Bi_3F_{10} \xrightarrow[-NH_4F]{285°C} 3\ BiF_3 \quad [1]$$

$$3\ BiF_3 + 4\ NH_3 \xrightarrow[30h]{285°C} Bi_3NF_6 + 3\ NH_4F \quad [2]$$

Upon longer reaction times at 285°C, partial hydrolysis by traces of water occurs and nonstoichiometric rhombohedral compounds BiO_xF_{3-2x} (x = 0.5 − 0.65) with the space group $R\bar{3}m$ or $R\bar{3}$, and a = 410 and c = 2026 pm (x = 0.55) are formed in addition to Bi_3NF_6.

Bi_3NF_6 decomposes under NH_3 at 350°C to Bi metal (Eq. [3]), while under an atmosphere of dry N_2 at 510°C BiF_3 and Bi are obtained (Eq. [4]):

$$2\ Bi_3NF_6 + 16\ NH_3 \rightarrow 6\ Bi + 3\ N_2 + 12\ NH_4F \quad [3]$$

$$2\ Bi_3NF_6 \rightarrow 4\ BiF_3 + 2\ Bi + N_2. \quad [4]$$

Bi_3NF_6 is a moisture-sensitive grey compound hydrolyzing within a few hours to $BiO_{0.5}F_2$. The i.r. spectrum shows absorptions at 588 cm^{-1} (w), 533 cm^{-1} (m), 492 cm^{-1} (vs), and 406 cm^{-1} (w).

Discussion of the Structure

Bi_3NF_6 belongs to the family of fluorite-type related compounds with anion excess. Within these compounds the anion excess can be accommodated by a local transformation of the primitive cubic lattice of anions to a close packing which may either occur in small clusterlike areas like in the structure of the mineral tveitite, $Ca_{14}Y_5F_{43}$ (M_nX_{2n+5}, n = 19) (16) and in KY_3F_{10} (15), or in two-dimensional sections like in the vernier phases M_nX_{2n+1} (17). In the latter the square 4^4-nets of anions are partially transformed to a denser triangular 3^6-net. This situation fits best for the member with n = 6, where six rows of the 4^4-net coincide almost exactly with seven rows of a parallel 3^6-net, with the exact relation being 6 : 6.93. The misfit is becoming larger the smaller the value of n in M_nX_{2n+1}, and the smallest value of n so far observed was n = 4, e.g., represented in Eu_4Cl_9 (18) and $Zr_4ON_3F_5$ (2). The misfit of 4 : 4.33 between the alternating 3^6 and 4^4-nets is either accommodated by the introduction of antiphase boundaries at the unit cell level like in the case of Eu_4Cl_9 or by ordering of anions of different size like N^{3-} and F^- in $Zr_4ON_3F_5$. Another possibility is a puckering of the 3^6-net which can be observed in most cases.

Bi_3NF_6 also forms a vernier phase, and it is besides $Lu_3O_2F_5$ (19) the first member with n = 3, showing the highest densification yet obtained.

While $Lu_3O_2F_5$ exhibits antiphase boundaries, Bi_3NF_6 does not (Fig. 3). This is astonishing as the low content of N atoms cannot compensate the large misfit of 3 : 3.464. The misfit is, however, partially balanced by an elongation of the square 4^4-net in the direction of the long crystallographic axis c which corresponds to 3 · 617.0 = 1851.13 pm in comparison with a = 581.7 pm and b = 570.2 pm (Table 1). Whereas for the other known vernier phases with $n > 3$, the superstructure is always an almost exact multiple of the two short axes or even less than that. In the case of $Lu_3O_2F_5$ the superstructure also shows an elongation. Its longest axis b = 3 · 562.5 pm has to be compared with a = 554.4 pm, and c = 529.2 pm (19).

In addition to the elongation in the direction of the superstructure, a strong puckering of the 3^6-net is present

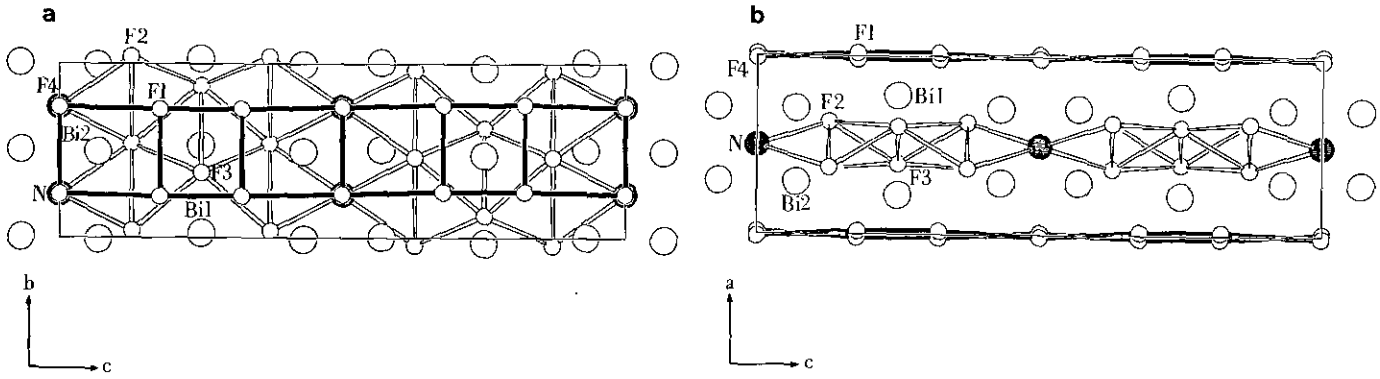

FIG. 3. Crystal structure of Bi_3NF_6 in projection along [100] and [010].

(Fig. 3) and it can be assumed that strong covalent Bi–N bonds of 225 and 227 pm also stablize the superstructure.

The N atoms are tetrahedrally coordinated by four Bi atoms, with the Bi_4N tetrahedra sharing edges to form linear chains along [010]. The parallel chains of tetrahedra are located in layers at the levels $z = 0$ and $z = 1/2$. Between these layers, slabs of a YF_3-type structure in which BiF_3 crystallizes are inserted at $z = 1/4$ and $z = 3/4$.

A slight structural change between the structures of YF_3 (20), BiF_3 (21), and the BiF_3-type slabs in Bi_3NF_6 can be visualized by the ratio of the crystallographic axes a and c of the orthorhombic YF_3-type structure. While this ratio is 1.44 for YF_3, it decreases to 1.36 for BiF_3, and 1.02 for the BiF_3-type slabs in Bi_3NF_6, which is close to the expected value for the cubic fluorite-type structure.

The atoms Bi(1) in the BiF_3-type slabs exhibit an eightfold coordination in form of a bicapped trigonal prism BiF_8 (Fig. 4), with the distances Bi(1)–F being in two ranges of three shorter ones between 221 and 226 pm and five longer ones between 240 and 244 pm (Table 3). The three closer F atoms together with the Bi atom form a trigonal pyramidal arrangement.

The atom Bi(2) also has three narrow neighbors in a pyramidal arrangement, two N atoms with distances 225

TABLE 3
Selected Bond Lengths in pm with Estimated Standard Deviations

Bi(1) – F(3)	221.3(6)	Bi(2) – N'	224.7(4)
Bi(1) – F(1)	226.3(5) (2×)	Bi(2) – N	227.6(4)
Bi(1) – F(3')	240.2(6)	Bi(2) – F(2)	225.4(4)
Bi(1) – F(2)	242.7(4) (2×)	Bi(2) – F(4)	249.5(5)
Bi(1) – F(1')	243.9(5) (2×)	Bi(2) – F(4')	262.2(4)
		Bi(2) – F(2')	285.2(6)
Bi(1) – F(3'')	369.2(6)	Bi(2) – F(1)	292.3(4)
		Bi(2) – F(1')	307.8(5)
		Bi(2) – F(2'')	332.7(6)

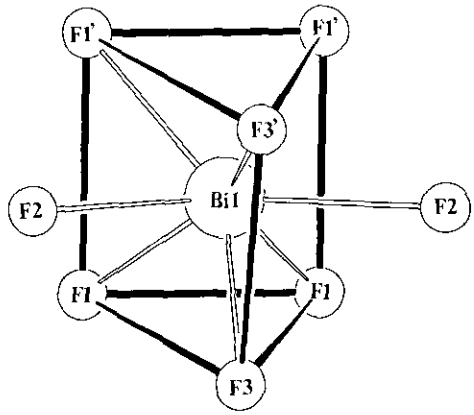

FIG. 4. Coordination polyhedron of Bi(1).

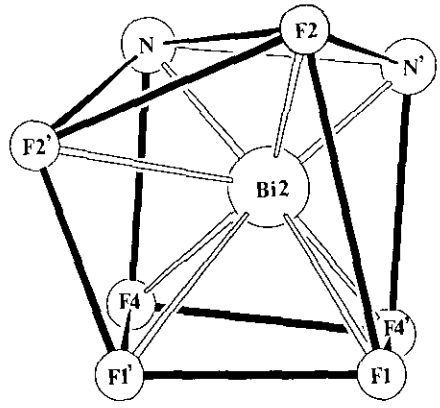

FIG. 5. Coordination polyhedron of Bi(2).

and 227 pm, and one F atom with 225 pm. In contrast to the coordination of Bi(1), the longer distances starting with Bi(2)–F = 249 pm increase almost continuously. Therefore, the first coordination sphere cannot unambiguously be determined. If, however, the first largest gap between the distances of 307.8 and 332.7 pm is taken as termination, then a coordination number of eight results, and the coordination polyhedron may be described as a distorted cube with one edge (F2–F2′) being displaced (Fig. 5).

ACKNOWLEDGMENTS

Financial support of the Deutsche Forschungsgemeinschaft and the Deutscher Akademischer Austauschdienst is gratefully acknowledged. The neutron diffraction and part of the X-ray diffraction experiments were carried out under the assistance and support of the ISIS Science Division at the Rutherford Appleton Laboratory. M. H. gives thanks for a scholarship of the E.C.

REFERENCES

1. C. Wüstefeld, T. Vogt, U. Löchner, J. Strähle, and H. Fuess, *Angew. Chem.* **100,** 1013 (1988); *Angew. Chem. Int. Ed. Engl.* **27,** 929 (1988).
2. R. Schlichenmaier, E. Schweda, J. Strähle, and T. Vogt, *Z. Anorg. Allg. Chem.* **619,** 367 (1993).
3. C. Wüstefeld, Thesis, Tübingen (1990).
4. T. Vogt, E. Schweda, J. P. Laval, and B. Frit, *J. Solid State Chem.* **83,** 324 (1989).
5. B. Tanguy, M. Pezat, J. Portier, and P. Hagenmuller, *Mater. Res. Bull.* **6,** 57 (1971).
6. R. Schlichenmaier, Thesis, Tübingen (1992).
7. C. Depierrefixe, Diplôme d'Etudes Approfondies, Limoges (1978).
8. J. Rodriguez-Carvajal, FullProf, version 2.2, June 1992, ILL, Grenoble.
9. M. A. Estermann and V. Gramlich, *J. Appl. Crystallogr.* **26,** 396 (1993).
10. M. J. Buerger, "Vector Space," Wiley, New York, 1959.
11. P. G. Simpson, R. D. Dobrott, and W. Lipscomb, *Acta Crystallogr.* **18,** 169 (1965).
12. Neutron diffractometer Polaris, ISIS, Rutherford Appleton Laboratory, Chilton, England.
13. TF15LS, Fotran program for the Rietveld refinement of TOF neutron powder diffraction data, ISIS Science Division, Rutherford Appleton Laboratory, Chilton, England (1993).
14. I. D. Brown and D. Altermatt, *Acta Crystallogr., Sect. B* **41,** 244 (1985).
15. J. W. Pierce and H. Y. P. Hong, "Proceedings 10th Rare Earth Conf., Carefree, Arizona **A2,** 527, 1973.
16. D. J. M. Bevan, J. Strähle, and O. Greis, *J. Solid State Chem.* **44,** 75 (1982).
17. B. G. Hyde, A. N. Bagshaw, S. Andersson, and M. O'Keeffe, *Ann. Rev. Mater. Sci.* **4,** 43 (1974).
18. R. Bachmann, Thesis, Karlsruhe (1987).
19. J. P. Laval, A. Taoudi, A. Abaouz, and B. Frit, *J. Solid State Chem.*, in press.
20. A. Zalkin, and D. H. Templeton, *J. Am. Chem. Soc.* **75,** 2453 (1953).
21. O. Greis and M. Martinez-Ripoll, *Z. Anorg. Allg. Chem.* **436,** 105 (1977).
22. C. Caglioti, A. Paoletti, and F. R. Ricci, *Nucl. Instrum. Methods* **3,** 223 (1958).
23. W. I. F. David, R. M. Ibberson, and J. C. Matthewman, Rutherford Appleton Laboratory Report No. 92-032 (1992).